www.elsevier.com/locate/jssc

High-pressure synthesis and crystal structures of the strontium oxogallates $Sr_2Ga_2O_5$ and $Sr_5Ga_6O_{14}$

Volker Kahlenberg, Valerie Goettgens, Philipp Mair, Daniela Schmidmair

PII: S0022-4596(15)00149-8
DOI: http://dx.doi.org/10.1016/j.jssc.2015.04.016
Reference: YJSSC18869

To appear in: *Journal of Solid State Chemistry*

Received date: 24 January 2015
Revised date: 5 April 2015
Accepted date: 12 April 2015

Cite this article as: Volker Kahlenberg, Valerie Goettgens, Philipp Mair, Daniela Schmidmair, High-pressure synthesis and crystal structures of the strontium oxogallates $Sr_2Ga_2O_5$ and $Sr_5Ga_6O_{14}$, *Journal of Solid State Chemistry*, http://dx.doi.org/10.1016/j.jssc.2015.04.016

High-pressure synthesis and crystal structures of the strontium oxogallates $Sr_2Ga_2O_5$ and $Sr_5Ga_6O_{14}$

Volker Kahlenberg[1,*], Valerie Goettgens[1], Philipp Mair[1] and Daniela Schmidmair[1]

[1]Institute of Mineralogy and Petrography, University of Innsbruck, Innrain 52, A-6020 Innsbruck, Austria

*Mailing Address: Volker Kahlenberg (corresponding author)
Institut für Mineralogie und Petrographie
Leopold-Franzens-Universität Innsbruck
Innrain 52
A- 6020 Innsbruck

E-mail : volker.kahlenberg@uibk.ac.at

Running title: On the crystal structures of $Sr_2Ga_2O_5$ and $Sr_5Ga_6O_{15}$

Keywords: System SrO-Ga_2O_3, $Sr_2Ga_2O_5$, $Sr_5Ga_6O_{14}$, high-pressure synthesis, single-crystal diffraction

Abstract

High-pressure synthesis experiments in a piston-cylinder apparatus at 1.5GPa / 3.0GPa and 1000°C resulted in the formation of single-crystals of $Sr_2Ga_2O_5$ and $Sr_5Ga_6O_{14}$, respectively. The structures of both compounds have been solved from single-crystal diffraction data sets using direct methods. The first compound is orthorhombic with space group type *Pbca* (*a* = 10.0021(4) Å, *b* = 9.601(4) Å, *c* = 10.6700(4) Å, *V* = 1024.6(4) Å^3, M_r = 394.68 u, *Z* = 8, D_x = 5.12 g/cm^3) and belongs to the group of single layer gallates. Individual sheets are parallel to (001) and can be built from the condensation of unbranched *vierer* single chains running along [010]. The layers are characterized by the presence of four- and strongly elliptical eight-membered rings of corner connected tetrahedra in *UUDD* and *UUUUDDDD* conformation. Strontium atoms are sandwiched between the tetrahedral layers for charge compensation and are coordinated by six and seven oxygen ligands, respectively. $Sr_2Ga_2O_5$ is isotypic with several other double sulfides and selenides. To the best of our knowledge, it is the first example of an oxide with this structure type. From a structural point of view, $Sr_5Ga_6O_{14}$ is a phyllogallate as well. The crystal structure adopts the monoclinic space group $P2_1/c$ (*a* = 8.1426(3) Å, *b* = 8.1803(3) Å, *c* = 10.8755(4) Å, β = 91.970(4)° *V* = 723.98(5) Å^3, M_r = 1080.42 u, *Z* = 2, D_x = 4.96 g/cm^3). Individual sheets extend along (001). Basic building units are unbranched *dreier* single chains parallel to [100]. The layers contain tertiary (Q^3) und quaternary (Q^4) connected [GaO_4]-tetrahedra in the ratio 2:1 resulting in a Ga:O ratio of 3:7 and the formation of exclusively five-membered rings. Linkage between adjacent tetrahedral sheets is provided by three symmetrically independent strontium ions which are surrounded by six to eight oxygen atoms. The layers in $Sr_5Ga_6O_{14}$ are similar to those observed in the melilite structure-type. Crystallochemical relationships between the present phases and other known compounds are discussed in detail.

Introduction

The phase relationships in the system SrO-Ga_2O_3 have been the subject of several experimental [1-3] as well as theoretical studies [4]. Apart from investigations related to the fundamental understanding of the thermodynamic properties of the strontium gallates, they have been also studied in the field of applied inorganic chemistry as potential host materials for rare earth element ions for the production of luminophors [5,6] or as sinter additives [7], for example. So far, the existence of the following seven different phases has been proved by crystal structure analysis: $SrGa_{12}O_{19}$ [8], $SrGa_4O_7$ [9], $SrGa_2O_4$ [10,11], $Sr_3Ga_4O_9$ [12], $Sr_3Ga_2O_6$ [13], $Sr_{10}Ga_6O_{19}$ [13-15] and $Sr_4Ga_2O_7$ [16]. Despite their chemical simplicity, the structure determinations of many of these compounds involved the solution of challenging crystallographic problems due to poor quality single-crystals adopting low symmetry structures with comparatively large unit cell volumes, polymorphism, complex twinning phenomena and incommensurate modulations.

In the literature, $Sr_2Ga_2O_5$ has been mentioned as a “low melting point oxide” that can be used for the ease of sintering of ceria [7,17] or stabilized ZrO_2 ceramics [18]. However, a more detailed examination reveals that the authors reporting about $Sr_2Ga_2O_5$ refer to the stoichiometric composition of the starting material and *not* to the chemical composition of a specific phase. Indeed, in the above-cited phase analytical studies no strontium gallate with a SrO:Ga_2O_3 ratio of 2:1 has been reported and quite recent synthesis experiments aiming on the preparation of brownmillerite-type $Sr_2Ga_2O_5$ at ambient pressure were also unsuccessful [19].

On the other hand, brownmillerites based on main group II and III elements have been already obtained by introducing pressure as an additional synthesis parameter. Examples include

$Ca_2Al_2O_5$ [20], Ca_2AlGaO_5 [21] and $Ca_2Ga_2O_5$ [22], respectively. In the course of an ongoing project on the crystal chemistry of brownmillerite-related compounds we tried to prepare the corresponding strontium equivalent at 1000°C and 1.5 GPa as well as 3.0 GPa using a piston-cylinder press. The present paper reports the first results of these investigations including the structural characterization of two previously unknown quenchable high-pressure double oxides of the system SrO-Ga_2O_3.

Experimental details

Polycrystalline starting material for the synthesis experiments was produced from mixtures of dried $SrCO_3$ (Fluka, purum) and Ga_2O_3 (Alfa Aesar, 99.99%) corresponding to a molar ratio of 2:1. The educts were carefully homogenized in an agate mortar under acetone. About 0.5 g of the reagents were subsequently pressed into discs having a diameter of 12mm and a thickness of 2 mm. The pellets confined in an open platinum crucible were heated in air from 300°C to 1100°C with a ramp of 60°C/min. The sample was held at this final temperature for 24 h and quenched in air. Weight loss was determined from weight differences before and after heating and corresponded to the theoretical value due to release of CO_2. A small part of the sintered precursor was used for X-ray powder diffraction which revealed the presence of $Sr_3Ga_2O_6$ and $Sr_3Ga_4O_9$, a result which is in agreement with the published phase diagrams [1-4]. The remaining material was stored in a desiccator.

High-pressure experiments were performed in an end-loaded piston-cylinder apparatus using 12.7 mm diameter graphite-NaCl furnace assemblies. Each 0.04 g of the precursor were sealed into 10 mm long Pt-capsules (outer diameter: 3.0 mm, thickness: 0.2 mm). Since pre-

experiments had revealed that the presence of moisture triggered the formation of hydrous phases, sample preparation of the slightly hygroscopic precursor including filling of the capsules was performed in a glove bag under nitrogen atmosphere. Subsequently, the closed container was packed in NaCl and placed vertically into the graphite furnace. Synthesis was conducted at 1.5 GPa as well as 3.0 GPa and 1000 °C. Pressure and temperature were monitored using a Heise pressure gauge and a Ni-CrNi thermocouple, respectively. After 72 h the sample was quenched isobarically by turning off the power of the furnace. Quench rates were of the order of 30 °C per second. After removal from the platinum tube the sample was transferred to a glass slide under a polarizing binocular microscope. A first optical inspection of the material prepared at 1.5 GPa revealed the existence of colourless-transparent optically isotropic and anisotropic crystals up to 200µm (diameter), indicating the presence of at least two different phases. Anisotropic crystals showing sharp extinction when imaged between crossed polarisers as well as isotropic samples were screened for further structural investigations. Therefore, several single-crystals were fixed on glass fibres using fingernail hardener as glue and diffraction data were collected on an Oxford Diffraction Gemini R Ultra single-crystal diffractometer. Preliminary diffraction experiments aiming on the determination of the unit cell parameters indicated that the isotropic samples correspond to NaCl-type strontium oxide. Among the anisotropic crystals two different compounds could be distinguished. Their diffraction patterns could be explained with orthorhombic (phase I) and monoclinic (phase II) primitive unit cells, respectively. In the sample synthesized at 3.0 GPa only crystals of phase I could be found. The results concerning the phase content of the two high-pressure runs were corroborated by X-ray powder diffraction experiments (see Figure 1a and b). The corresponding powder diffraction

data were recorded on a Bruker D8-Discover diffractometer using a Cu-tube operated at 40 kV and 40 mA. The device is equipped with a primary-beam germanium monochromator yielding Cu$K\alpha_1$ radiation and a LYNXEYE^{TM} silicon strip detector. Data were collected in Bragg-Brentano geometry with θ-2θ-coupling at ambient temperature in the 2θ range between 2-90° with a counting time of 2 s per step and a step size of 0.01°θ. Due to the limited amount of material the carefully grounded sample was prepared on a "background-free" sample holder consisting of the polished surface of a specially cut silicon single-crystal. During the measurements sample rotation was activated. Phase analysis was based on LeBail-fits which were carried out using the TOPAS 4.2 [23] software suite. Peak shapes were calculated via the fundamental parameter approach. Notably, in case of $Sr_5Ga_6O_{14}$ a pronounced anisotropic peak broadening was observed which required the application of spherical harmonics up to 6th order to describe the peak width as a function of (*hkl*) properly.

For both phases I and II, a search of the recent WEB-based version 3.1.0 of the *Inorganic Crystal Structure Database* using a combination of the unit cell parameters and the expected chemical elements did not yield any hits and, therefore, we finally decided to collect data sets for structure determination. Intensities corresponding to one hemisphere of reciprocal space were acquired for each phase at 298(2) K with ω-scans of 1.0° scan width per frame. Subsequent integration and data reduction was performed with the *CrysAlis Pro* software package [24]. Data reduction included Lorentz and polarization corrections and an analytical absorption correction based on the procedure of Clark and Reid [25] using accurately measured external faces. In both cases, the analysis of the systematic absences allowed the unequivocal determination of the space group type: *Pbca* (for phase I) and $P2_1/c$ (for phase II), respectively.

Structure solution by direct methods (program SIR92, [26]) resulted in crystallochemically reasonable models, i.e. gallium atoms tetrahedrally coordinated by four oxygen ligands and additional strontium positions. The derived charge neutral chemical compositions are as follows: $Sr_2Ga_2O_5$ (phase I) and $Sr_5Ga_6O_{14}$ (phase II), respectively. Subsequent refinement calculations were performed using the program SHELX-97 [27] within the WinGX program suite [28]. X-ray scattering factors for neutral atoms together with real and imaginary coefficients for anomalous dispersion were taken from the *International Tables for Crystallography, Vol. C* [29]. The final least-squares calculations including anisotropic displacement parameters and a Larson-type [30] secondary extinction correction resulted in the following residuals: $R1$=0.021 for $Sr_2Ga_2O_5$ (838 independent observed reflections, 83 variable parameters) and $R1$=0.026 for $Sr_5Ga_6O_{14}$ (1205 independent observed reflections, 116 variable parameters). In each case the largest shift/esd. in the final cycle was < 0.001. A summary of all relevant information concerning data collection and refinement can be found in Table 1. The optimized atomic coordinates, equivalent isotropic and anisotropic displacement factors as well as selected interatomic distances and angles are given in Tables 2 to 4. Figures showing structural details were made using the program ATOMS6.4 [31]. Further details of the crystal structure investigations may be obtained from Fachinformationszentrum Karlsruhe, 76344 Eggenstein-Leopoldshafen, Germany (fax: (+49)7247-808-666; e-mail: crysdata@fiz-karlsruhe.de) on quoting the deposition numbers CSD-428803 (for $Sr_2Ga_2O_5$) and CSD-428804 (for $Sr_5Ga_6O_{14}$), respectively.

Results

$Sr_2Ga_2O_5$

The crystal structure of $Sr_2Ga_2O_5$ belongs to the group of single layer gallates. Using the nomenclature introduced by Liebau [32] the more detailed crystallochemical formula can be written as $Sr_2\{\boldsymbol{uB},4,1^2_\infty\}Ga_2O_5$. A single tetrahedral layer parallel to (001) can be built from the condensation of strongly folded unbranched *vierer* single chains (see Figure 2). One discrete chain is running along [010] and has a translation period of about 9.60 Å. Condensation of two neighboring chains, which are related by inversion centers, produces a band which is characterized by the simultaneous presence of four- and strongly elliptical eight-membered rings of corner connected tetrahedra. Further condensation of the bands via bridging oxygens results in the sheets mentioned above. The sequence of directedness of "up" (*U*) and "down" (*D*) pointing tetrahedra in the rings is as follows: *UUDD* and *UUUUDDDD*, respectively.

Each layer contains exclusively tertiary (Q^3) tetrahedra, i.e. the Ga:O ratio is 2:5. The Ga-O distances of the two crystallographically independent tetrahedra within the asymmetric unit range from 1.823 to 1.881 Å. As one would expect, distances between the gallium cations and the terminal oxygen ligands O(1) and O(3) are the shortest Ga-O distances. The O-Ga-O angles show a significant scatter throughout both polyhedra. Nevertheless, the values are within the expected limits for oxogallates [12-16]. Distortion parameters (quadratic elongation, bond variances, [33]) for the tetrahedra are listed in Table 3a. The vertex symbols for both tetrahedral centers are the same: $8_2.4_1$. A schematic representation of the arrangement of the rings within a single layer is given in Figure 3.

Strontium atoms are sandwiched between the tetrahedral layers. They are coordinated by six (for Sr(1)) and seven (for Sr(2)) oxygen ligands, respectively. The corresponding coordination polyhedra can be approximately described as octahedra (around Sr(1)) and pentagonal

bipyramids (around Sr(2)). These strontium-centered units are linked into sheets, where every octahedron shares four corners with neighboring octahedra and two edges as well as one face with adjacent bipyramids. A single bipyramid in turn shares four corners with other bipyramids and two edges as well as two faces with surrounding octahedra (see also Figure 4).

Bond valence sums calculations based on the parameter sets of Brese & O'Keeffe [34] for the Sr-O and Ga-O bonds resulted in values for the cations and anions that were close to the nominal charge values of 2 and 3 valence units, respectively (see Table 3a). A side view of the whole crystal structure is given in Figure 5.

$Sr_5Ga_6O_{14}$

$Sr_5Ga_6O_{14}$ can be also allocated as a single layer gallate based on sheets resulting from the condensation of [GaO_4]-units. Individual sheets extend on (001). The main building units of the layers are chains of corner sharing tetrahedra which can be classified as unbranched *dreier* single-chains (parallel to [100]), i.e. the structural formula [32] can be written as $Sr_5\{\boldsymbol{uB},3,1^2_\infty\}Ga_6O_{14}$ (see Figure 6). However, in contrast to $Sr_2Ga_2O_5$ where only Q^3-connected tetrahedra can be found, $Sr_5Ga_6O_{14}$ contains tertiary (Q^3) und quaternary (Q^4) connected moieties in the ratio 2:1 resulting in a different Ga:O ratio of 3:7. A single layer contains exclusively five-membered rings (see Figure 7). Two out of three Q^3-tetrahedra within a single ring are either "*U*" or "*D*". The remaining two Q^4-polyhedra have an "edge" or "*E*" orientation. The vertex symbols for the crystallographically independent Ga atoms are as follows: 5_3 (for Ga(2) and Ga(3)) and 5_4 (for Ga(1)).

The Ga-O bond distances in $Sr_5Ga_6O_{14}$ vary between 1.804 and 1.894 Å (Table 3b). They are in the normal range of oxogallate structures. Concerning the spread of individual Ga-O distances it can be noticed that the quaternary (Q^4) tetrahedra around Ga(1) sharing all four oxygen ligands with neighboring tetrahedra are the least distorted ones. In general, the bond-valence sums for the different crystallographic sites showed satisfactory agreement with the expected values (see Table 3b). However, larger deviations occur for the oxygen atoms O(6) (BVS = 1.659 v.u.) and O(5) (BVS = 2.287 v.u.), respectively. This pronounced under- and overbonding at ambient pressure reflects a steric strain in the crystal structure of $Sr_5Ga_6O_{14}$ and may be the explanation why high pressure is needed for its preparation. Linkage between adjacent tetrahedral layers as well as charge compensation is provided by three symmetrically independent strontium ions which are surrounded by six to eight oxygen atoms. A side view of the whole crystal structure is presented in Figure 8.

Discussion and comparison with related structures

The crystal structure of $Sr_2Ga_2O_5$ is isotypic with $Sr_2Ga_2S_5$, $Ba_2In_2S_5$ and $Ba_2In_2Se_5$ [35]. To the best of our knowledge, $Sr_2Ga_2O_5$ is the first example of an *oxide* with this structure type. For the calculation of several quantitative descriptors for the characterization of the degree of similarity between the crystal structures of $Sr_2Ga_2O_5$ and $Sr_2Ga_2S_5$, differing only in the type of the chalcogenide anion, the program COMPSTRU [36] was used. For the given two examples, the degree of lattice distortion (S), i.e. the spontaneous strain obtained from the eigenvalues of the finite Lagrangian strain tensor calculated in a Cartesian reference system, has a value of (S) = 0.0816, reflecting the comparatively large differences between the lattice parameters of the two structures due to the differences between the ionic radii of O^{2-} and S^{2-}. After a

transformation according to **a**' = **b**, **b**' = **c** and **c**' = **a** and an origin shift of (½,½,0) the structure of $Sr_2Ga_2S_5$ was mapped on the most similar configuration of $Sr_2Ga_2O_5$. Notably, this transformation does not change the Hermann-Mauguin symbol *Pbca* of the space group type. The calculations showed the following atomic displacements (in Å) between the corresponding atoms in the oxide (first entry) and the sulphide (second entry): Sr(1)-Sr(1): 0.574; Sr(2)-Sr(2): 0.354; Ga(1)-Ga(1): 0.229; Ga(2)-Ga(2): 0.407; O(1)-S(1): 0.491; O(2)-S(2): 0.370; O(3)-S(4): 0.311; O(4)-S(3): 0.289; O(5)-S(5): 0.583, i.e. the maximum displacement $d_{max.}$ is about 0.58 Å. The arithmetic mean is $d_{av.}$ = 0.401 Å. The measure of similarity Δ as defined by Bergerhoff *et al.* [37] has a value of 0.118.

Among the group of alkaline earth oxogallates, structures containing layers of four- and eight-membered rings have been observed in the β- and γ-polymorph of $SrGa_2O_4$ [10]. However, in these two phases the layered motifs occur as building units within a framework and not as isolated sheets within a "real" phyllogallate. A detailed list of the 17 topologically simplest ways of linking *UUDD* four-membered rings into a layer such that only eight-membered rings are build between them is listed in Liebau's classical survey on the structural chemistry of silicates [32]. The comparison with the layers observed in $Sr_2Ga_2O_5$ reveals, that they are topologically identical with those reported for the zeolite gismondine ($CaAl_2Si_2O_8{\cdot}4H_2O$, [38]). A genuine phyllosilicate with the same layer topology, for example, is cavansite ($Ca(VO)(Si_4O_{10}){\cdot}4H_2O$, [39]). However, the axial ratio ε of the longest and shortest diameter of the eight-membered rings - which can be used as a measure of their ellipticity - are quite different. Actually, the values increase drastically from ε = 1.25 (in gismondine) and ε = 1.75 (in cavansite) to 3.17 in $Sr_2Ga_2O_5$.

The tetrahedral layer observed in $Sr_5Ga_6O_{14}$ is a well known structural building unit which is characteristic for the melilite structure-type. Melilites are an important family of rock-forming silicate minerals and are usually described as a solid solution series between the end-members gehlenite ($Ca_2Al[AlSiO_7]$) and åkermanite ($Ca_2Mg[Si_2O_7]$) [40]. A single tetrahedral layer from the tetragonal åkermanite-structure containing corner sharing [SiO_4]- and [MgO_4]-units is given in Figure 9a. The close relationship with $Sr_5Ga_6O_{14}$ (see Figure 9b) is evident. Small distortions and tilts of the tetrahedra in the present compound are the reason for the lower overall layer symmetry: layer group $p\,\bar{4}\,2_1m$ (in melilite) and $p2_1$ (in $Sr_5Ga_6O_{14}$).
Notably, the melilite structure-type is also known among oxogallates. Examples include $(Sr_{0.5}La_{0.5})_2Ga_3O_7$ [41] or the incommensurately modulated compound $(Ca_{0.5}La_{0.5})_2Ga_3O_7$ [42]. Furthermore, the melilite-type solid solution series $La_{1+x}Sr_{1-x}Ga_3O_{7+x/2}$ has been studied intensively during the last years as an potential electrolyte in solid oxide fuel cells (SOFCs) [43-46].

Concerning the stacking sequence of the tetrahedral layers the melilite structure-type is simpler: adjacent sheets along the tetragonal *c*-axis are translationally equivalent, creating a …AAAA… sequence. The stacking sequence in $Sr_5Ga_6O_{14}$ comprises two layers (...ABABAB...) where subsequent sheets are related by inversion centres. 2_1-screw axes are running within the layers, i.e. they map a single layer onto itself (layer symmetry $p2_1$). The different stacking scheme results in the formation of different types of vacancies in $Sr_5Ga_6O_{14}$ where the Sr^{2+}-cations can be hosted in form of SrO_6-, SrO_7- and SrO_8-polyhedra. The large di- and trivalent cations in melilite have eight oxygen ligands.

Comparing the chemical formulas of melilite-type $(Sr_{0.5}La_{0.5})_2Ga_3O_7$ with $Sr_5Ga_6O_{14}$ (or $Sr_{2.5}Ga_3O_7$) it becomes obvious that in the latter phase additional cation positions must exist in the interspace between the tetrahedral layers. Whereas in melilite the non-tetrahedral cations exclusively reside on positions above and below the centres of the five-membered rings, in $Sr_5Ga_6O_{14}$ extra strontium ions are incorporated in the vicinity of the Q^4-tetrahedra (see Figure

9a and b). Furthermore, a slight shift of the Sr-ions away from the central positions is observed. It is interesting to note, that the above-mentioned pronounced underbonding of the non-bridging oxygen O(6) in $Sr_5Ga_6O_{14}$ is also observed for the corresponding O-atom in the crystal structure of $(Sr_{0.5}La_{0.5})_2Ga_3O_7$, although to a lesser extent (BVS: 1.729 v.u.).

Finally, we would like to point out that the chemically closely related ambient pressure oxogallate $Ca_5Ga_6O_{14}$ [47] is also based on the same type of melilite-like layers. However, the layer symmetry is slightly different (layer group *cm*). Stacking of the sheets via a 2_1-screw axis perpendicular to the layers again creates a ...ABABAB... sequence. The different stacking-type is reflected in the arrangement of the divalent cations in the interspace. From the comparison between Figures 9b and 9c it is evident that one of cation sites in the Sr-compound that was located above the centres of rings has almost completely moved away from central position, creating an almost "empty" ring in $Ca_5Ga_6O_{14}$.

The samples retrieved from the high-pressure studies consisted of three different phases: SrO, $Sr_5Ga_6O_{14}$ and $Sr_2Ga_2O_5$. Since the latter crystalline compound corresponds to the bulk composition of the ceramic precursor the following reaction mechanism can be assumed: SrO + $Sr_5Ga_6O_{14}$ → $3Sr_2Ga_2O_5$, i.e. in an initial step during the high-pressure high-temperature treatment at 1.5GPa and 1000°C the first two phases were formed from the precursor which in turn reacted to $Sr_2Ga_2O_5$. The comparison of the densities of the different phases (ρ_{SrO} = 5.03 g/cm^3 [48], $\rho_{Sr5Ga6O15}$ = 4.96 g/cm^3, $\rho_{Sr2Ga2O5}$ = 5.12 g/cm^3) as well as the calculation of the reaction volume ΔV_r = -7.16 cm^3 also support the suggested direction of the reaction. Therefore, the quenched high-pressure experiment at 1.5 GPa corresponds to an intermediate

state representing the incomplete formation of $Sr_2Ga_2O_5$ from the two other compounds. For the synthesis run at 3.0 GPa the above-mentioned reaction was complete.

Under the chosen experimental P-T conditions no brownmillerite-type phase was observed. Using literature data, however, the volume and density of this hypothetical $Sr_2Ga_2O_5$ polymorph can be at least estimated. $Sr_2In_2O_5$ [49] and $Sr_2Ga_{1.1}In_{0.9}O_5$ [19] both can be prepared at ambient pressure and adopt the body-centered brownmillerite variant with unit cell volumes of 556.7 and 518.6 $Å^3$, respectively. Assuming an ideal solid solution, i.e. a linear dependency of the lattice parameters from the chemical composition, the unit cell volume of the pure gallium end-member can be extrapolated at about 487.5 $Å^3$. The resulting density of 5.38 g/cm^3 is much higher than the observed value for the layered $Sr_2Ga_2O_5$ form (5.12 g/cm^3) indicating that the application of even higher pressures may stabilize the brownmillerite-type phase. To verify this hypothesis, piston-cylinder experiments at considerably higher pressures than the maximal 3.0 GPa used for the first runs are planned for the next future.

Acknowledgement

The authors would like to thank the three anonymous reviewers for their helpful comments and suggestions.

References

[1] C.W.W. Hoffman, J.J. Brown, Compound formation and Mn^{2+}-activated luminescence in the binary systems R_2O- and RO-Ga_2O_3. J. Inorg. Nucl. Chem. 30 (1968) 63-79.

[2] L.A. Plakhtii, N.S. Afonskii, Z. Ya. Pol'shchikova, L.M. Kovba, Strontium gallates. Russ. J. Inorg. Chem. 13 (1968) 634-635.

[3] V.P. Kobzareva, L.M. Kovba, L.M. Lopato, L.N. Lykova, A.V. Shevchenko, Equilibrium diagram of the SrO- Ga_2O_3 system. Russ. J. Inorg. Chem. 21 (1976) 903-904.

[4] M. Zinkevich, Calorimetric study and thermodynamic assessment of the SrO–Ga_2O_3 system. Int. J. Mat. Res. 98 (2007) 574-579.

[5] S.H.M. Poort, W.P. Blokpoel, G. Blasse, Luminescence of Eu^{2+} in barium and strontium aluminate and gallate. Chem. Mater. 7 (1995) 1547-1551.

[6] S.-H. Yang, H.-F. Tu, Novel $SrGa_2O_4$ phosphor for tunable blue-white luminescence. J. Electrochem. Soc. 152 (2005) H1-H5.

[7] J.-S. Lee, Effects of strontium gallate additions on sintering behaviour of gadolinia-doped ceria. J. Electroceram. 17 (2006) 709-711.

[8] K. Kimura, M. Ohgaki, K. Tanaka, H. Morikawa, F. Marumo, Study of the bipyramidal site in magnetoplumbite-like compounds, $SrM_{12}O_{19}$ (M=Al,Fe,Ga). J. Solid State Chem. 87 (1990) 186-194.

[9] H.J. Deiseroth, Hk. Müller-Buschbaum, Über Erdalkalioxogallate. II. Zur Kenntnis von $SrGa_4O_7$. Z. Anorg. Allg. Chem. 387 (1972) 154-160.

[10] V. Kahlenberg, R.X. Fischer, C.S.J. Shaw, Polymorphism of strontium monogallate: the framework structures of β-$SrGa_2O_4$ and ABW-type γ-$SrGa_2O_4$. J. Solid State Chem. 153 (2000) 294-300.

[11] A.R. Schulze, Hk. Müller-Buschbaum, Über Erdalkalioxogallate, IX. Zum Aufbau von β-$SrGa_2O_4$. Z. Naturforsch. 36b (1982) 892-893.

[12] V. Kahlenberg, J.B. Parise, $Sr_3Ga_4O_9$ - a strontium gallate with a new tetrahedral layer structure. Z. Kristallogr. 216 (2001) 210-214.

[13] V. Kahlenberg, The crystal structures of the strontium gallates $Sr_{10}Ga_6O_{19}$ and $Sr_3Ga_2O_6$. J. Solid State Chem. 160 (2001) 421-429.

[14] V. Kahlenberg, β-$Sr_{10}Ga_6O_{19}$: an oxygen deficient perovskite containing $[Ga_6O_{19}]$-polyanions. Solid State Sciences 4 (2002) 183-189.

[15] H. Krüger, B. Lazić, E. Arroyabe, V. Kahlenberg, Modulated structure and phase transitions of $Sr_{10}Ga_6O_{19}$. Acta Cryst. B 65 (2009) 587-592.

[16] V. Kahlenberg, B. Lazić, V. Krivovichev, Tetrastrontium-digalliumoxide ($Sr_4Ga_2O_7$) - synthesis and crystal structure of a mixed strontium gallate related to perovskite. J. Solid State Chem. 178 (2005) 1429-1439.

[17] S.-W. Seo, S.-J. Jung, M.-W. Park, S.-M. Yu, K.-T. Lee, J.-S. Lee, Effects of strontium gallate addition on sintering behavior and electrical conductivity of yttria-doped ceria. Electron. Mater. Lett. 10 (2014) 213-216.

[18] M. Feng, J.B. Goodenough, Improving stabilized zirconia with strontium gallate. J. Am. Ceram. Soc. 77 (1994) 1954-1956.

[19] S. Ya. Istomin, E.V. Antipov, Yu. S. Fedotov, S. I. Bredikhin, N.V. Lyskov, S. Shafeie, G. Svensson, Y. Liu, Z. Shen, Crystal structure and high-temperature electrical conductivity of novel perovskite-related gallium and indium oxides. J. Solid State Electrochem. 18 (2014) 1415-1423.

[20] V. Kahlenberg, R.X. Fischer, C.S.J. Shaw, Rietveld analysis of dicalcium aluminate ($Ca_2Al_2O_5$) – a new high pressure phase with the brownmillerite-type structure. Am. Mineral. 85 (2000) 1061-1065.

[21] V. Kahlenberg, C.S.J. Shaw, The crystal structure of the calcium aluminogallates $CaAlGaO_4$ and Ca_2AlGaO_5. J. Solid State Chem. 157 (2001) 62-67.

[22] V. Kahlenberg, C.S.J. Shaw, $Ca_2Ga_2O_5$: a high pressure oxogallate. Z. Kristallogr. 216 (2001) 206-209.

[23] Bruker-AXS (2009). TOPAS, Version 4.2: General Profile and Structure Analysis Software for Powder Diffraction Data; Bruker-AXS, Karlsruhe, Germany.

[24] Agilent (2012). *CrysAlis PRO*. Agilent Technologies, Yarnton, Oxfordshire, England.

[25] R.C. Clark, J.S. Reid, The analytical calculation of absorption in multifaceted crystals. Acta Cryst. A 51 (1995) 887-897.

[26] A. Altomare, G. Cascarano, C. Giacovazzo, A. Guagliardi, M.C. Burla, G. Polidori, M. Camalli, SIR92 - a program for automatic solution of crystal structures by direct methods. J. Appl. Cryst. 27 (1994) 435.

[27] G.M. Sheldrick (1997) SHELX-97 - A program for crystal structure refinement. University of Göttingen, Germany.

[28] L.S. Farrugia, WinGX suite for small-molecule single-crystal crystallography. J. Appl. Cryst. 32 (1999) 837-838.

[29] E. Prince, (ed.) (2004) International Tables for Crystallography, Vol. C: Mathematical, physical and chemical tables, third edition. Kluwer Academic Publishers, Dordrecht, Boston, London.

[30] A.C. Larson, Inclusion of secondary extinction in least-squares calculations. Acta Cryst. 23 (1967) 664-665.

[31] E. Dowty (2011) ATOMS6.4. Shape Software, Kingsport, USA.

[32] F. Liebau, Structural chemistry of silicates. Springer Verlag, Berlin 1985.

[33] K. Robinson, G.V. Gibbs, P.H. Ribbe, Quadratic elongation: a quantitative measure of distortion in coordination polyhedra. Science 172 (1971) 567-570.

[34] N.E. Brese, M. O'Keeffe, Bond-valence parameters for solids. Acta Cryst. B 47 (1991) 192-197.

[35] B. Eisenmann, A. Hofmann, Schichtionen in den Kristallstrukturen der isotypen Verbindungen $Sr_2[Ga_2S_5]$, $Ba_2[In_2S_5]$ und $Ba_2[In_2Se_5]$. Z. Anorg. Allg. Chem. 580 (1990) 151-159.

[36] E.S. Tasci, G. de la Flor, D. Orobengoa, C. Capillas, J.M. Perez-Mato, M.I. Aroyo, An introduction to the tools hosted in the Bilbao Crystallographic Server. EPJ Web of Conferences 22 (2012) 00009.

[37] G. Bergerhoff, M. Berndt, K. Brandenburg, T. Degen, Concerning inorganic crystal structure types. Acta Cryst. B 55 (1995) 147-156.

[38] R. Rinaldi, G. Vezzalini, Gismondine: the detailed x-ray structure refinement of two natural samples. Studies Surf. Sci. Catal. 24 (1985) 481-492.

[39] J.M. Hughes, R.S. Derr, F. Cureton, C.F. Campana, G. Druschel, The crystal structure of cavansite: location of the H_2O molecules and hydrogen atoms in $Ca(VO)(Si_4O_{10})\cdot H_2O$. Can. Mineral. 49 (2011) 1267-1272.

[40] I.P. Swainson, M.T. Dove, W.W. Schmahl, A. Putnis, Neutron powder diffraction study of the åkermanite-gehlenite solid solution series. Phys. Chem. Minerals 19 (1992) 185-195.

[41] M. Steins, W. Schmitz, R. Uecker, J. Doerschel, Crystal structure of strontium trigallium heptoxide $(Sr_{0.5}La_{0.5})Ga_3O_7$. Z. Kristallogr. NCS 212 (1997) 76.

[42] F. Wei, T. Baikie, T. An, C. Kloc, J. Wei, T. White, Crystal chemistry of melilite $[CaLa]_2[Ga]_2[Ga_2O_7]_2$: a five dimensional solid electrolyte. Inorg. Chem. 51 (2012) 5941-5949.

[43] A. Mancini, V. Felice, I.N. Sora, L. Malavasi, Chemical compatibility study of melilite-type gallate solid electrolyte with different cathode materials. J. Solid State Chem. 213 (2014) 287-292.

[44] M. Rozumek, P. Majewski, H. Schluckwerder, F. Aldinger, Electrical conduction behavior of $La_{1+x}Sr_{1-x}Ga_3O_{7-\square}$ melilite-type ceramics. J. Am. Ceram. Soc. 87 (2004) 1795-1798.

[45] X. Kuang, M.A. Green, H. Niu, P. Zajdel, C. Dickinson, J.B. Claridge, L. Jantsky, M.J. Rosseinsky, Interstitial oxide ion conductivity in the layered tetrahedral network melilite structure. Nat. Mater. 7 (2008) 498-504.

[46] C.I. Thomas, X. Kuang, Z. Deng, H. Niu, J.B. Claridge, M.J. Rosseinsky, Phase stability control of the interstitial oxide ion conductivity in the $La_{1+x}Sr_{1-x}Ga_3O_{7+x/2}$ melilite family. Chem. Mater. 22 (2010) 2510-2516.

[47] A.I. Bilyi, V.A. Bruskov, J.N. Grin, P.J. Zavalij, V.V. Kravchishin, A.E. Nosenko, Crystal structure of $Ca_5Ga_6O_{14}$ (in Russian). Kristallografiya 31 (1986) 1217-1219.

[48] W.G. Burgers, Röntgenographische Untersuchungen des Verhaltens von BaO-SrO Gemischen beim Glühen. Z. für Physik 80 (1933) 352-360.

[49] R. von Schenck, Hk. Müller-Buschbaum, Über ein neues Erdalkalimetall-Oxoindat: $Sr_2In_2O_5$. Z. Anorg. Allg. Chem. 395 (1973) 280-286.

Figure captions

Figure 1. Observed X-ray powder diffraction patterns and the corresponding LeBail-fits of the samples prepared at (a) 1.5 and (b) 3.0 GPa. For the 1.5 GPa synthesis calculated step intensities (red line) have been modeled based on a mixture of three different phases: black, pink and green tick marks correspond to $Sr_2Ga_2O_5$, $Sr_5Ga_6O_{14}$ and SrO, respectively. The 3.0 GPa sample consists of almost phase pure $Sr_2Ga_2O_5$. Three low intensity reflections marked with arrows are probably due to an unidentified impurity. The blue lines at the bottom of each diagram represent the difference curves between observed and calculated step intensities.

Figure 2. Single tetrahedral layer in $Sr_2Ga_2O_5$ in a projection parallel to [001]. Strongly folded unbranched *vierer* single chains are running parallel to [010].

Figure 3. Topology of a single layer in $Sr_2Ga_2O_5$ with four- and eight-membered rings.

Figure 4. Arrangement of the SrO_6- (blue) and SrO_7-polyhedra (yellow) in $Sr_2Ga_2O_5$ in the interspace between the tetrahedral layers.

Figure 5. Side view of the whole crystal structure of $Sr_2Ga_2O_5$. Large blue spheres represent the strontium cations.

Figure 6. Single tetrahedral layer in $Sr_5Ga_6O_{14}$ in a projection perpendicular to the sheets. Unbranched *dreier* single chains are running parallel to [100].

Figure 7. Topology of a single layer in $Sr_5Ga_6O_{14}$ with five-membered rings.

Figure 8. Side view of the whole crystal structure of $Sr_5Ga_6O_{14}$. Large spheres represent the strontium cations.

Figure 9. Comparison between the tetrahedral layers and the location of the cations in the interspace directly above the sheets in (a) melilite, (b) $Sr_5Ga_6O_{14}$ and (c) $Ca_5Ga_6O_{14}$.

Table 1. Crystal data and structure refinement for the two high-pressure strontium gallates.

Crystal-cell data		
Empirical formula	$Sr_2Ga_2O_5$	$Sr_5Ga_6O_{14}$
Formula weight	394.68	1080.42
Temperature	298(2) K	
Wavelength	0.71073 Å	
Crystal system	Orthorhombic	Monoclinic
Space group	*Pbca*	$P2_1/c$
Unit cell dimensions	a = 10.0021(4) Å	a = 8.1426(3) Å
	b = 9.601(4) Å	b = 8.1803(3) Å
	c = 10.6700(4) Å	c = 10.8755(4) Å
		β = 91.970(4)°
Volume	1024.6(4) $Å^3$	723.98(5) $Å^3$
Z	8	2
Density (calculated) g/cm^3	5.117	4.956
Absorption coefficient	31.046 mm^{-1}	29.298 mm^{-1}
F(000)	1424	976
Intensity measurements		
Crystal size	0.16 x 0.16 x 0.05 mm^3	0.10 x 0.08 x 0.07 mm^3
Theta range for data collection	3.51 to 25.34°	3.12 to 25.34°
Diffractometer	Oxford Diffraction Gemini R Ultra	
Monochromator	Graphite	
Index ranges	-12<=h<=12, -11<=k<=10, -10<=l<=12	-9<=h<=8, -8<=k<=9, -10<=l<=13

Scan type	ω-scans	
Scan width	1 °	
Exposure time	22.5 s / frame	30 s / frame
Reflections collected	5436	4267
Independent reflections	936 [R(int) = 0.0417]	1315 [R(int) = 0.0277]
Observed reflections [I>2sigma(I)]	838	1205
Completeness to theta = 25.34°	100.0 %	99.6 %
Max. and min. transmission	0.3059 and 0.0828	0.2336 and 0.1577
Refinement of the structures		
Refinement method	Full-matrix least-squares on F^2	
Parameters / restraints	83 / 0	116 / 0
Goodness-of-fit on F^2	1.166	0.998
Final R indices [I>2σ(I)]	R1 = 0.021, wR2 = 0.050	R1 = 0.026, wR2 = 0.066
R indices (all data)	R1 = 0.026, wR2 = 0.052	R1 = 0.029, wR2 = 0.068
Extinction coefficient	0.00155(8)	0.0022(3)
Largest diff. peak and hole	0.769 and -0.632 e.Å^{-3}	0.917 and -1.067 e.Å^{-3}

Table 2a. Atomic coordinates (x 10^4) and equivalent isotropic displacement parameters ($Å^2$x 10^3) for $Sr_2Ga_2O_5$. U(eq) is defined as one third of the trace of the orthogonalized U_{ij} tensor. Bond valence sums (BVS) have been calculated using the data sets of Brese & O'Keeffe [32].

	x	y	z	U(eq)	BVS
Sr(1)	35(1)	44(1)	2444(1)	8(1)	1.903
Sr(2)	2454(1)	2484(1)	2255(1)	7(1)	1.936
Ga(1)	9665(1)	2673(1)	57(1)	5(1)	2.872
Ga(2)	7336(1)	390(1)	308(1)	6(1)	2.863
O(1)	7626(3)	-90(3)	1939(3)	8(1)	2.010
O(2)	8805(3)	1081(4)	-580(3)	8(1)	1.917
O(3)	9866(3)	2566(3)	1758(3)	8(1)	1.908
O(4)	8622(3)	4109(4)	-618(3)	9(1)	1.931
O(5)	11306(3)	3014(4)	-637(3)	14(1)	1.808

Table 2b. Atomic coordinates (x 10^4) and equivalent isotropic displacement parameters ($Å^2$x 10^3) for $Sr_5Ga_6O_{14}$ U(eq) is defined as one third of the trace of the orthogonalized U_{ij} tensor. Bond valence sums (BVS) have been calculated using the data sets of Brese & O'Keeffe [32].

	x	y	z	U(eq)	BVS
Sr(1)	0	5000	0	15(1)	1.904
Sr(2)	4070(1)	2452(1)	19(1)	8(1)	1.744
Sr(3)	1585(1)	9070(1)	9708(1)	14(1)	2.144
Ga(1)	7311(1)	4133(1)	2465(1)	6(1)	2.933
Ga(2)	6140(1)	586(1)	2885(1)	6(1)	2.952
Ga(3)	8964(1)	7708(1)	2614(1)	5(1)	2.896
O(1)	6616(6)	2621(5)	3602(4)	10(1)	1.926

O(2)	8353(6)	5775(5)	3377(4)	13(1)	1.952
O(3)	7727(5)	9183(5)	3488(4)	10(1)	2.052
O(4)	5762(6)	4894(6)	1351(4)	10(1)	1.854
O(5)	8979(5)	3172(6)	1618(4)	9(1)	2.287
O(6)	8957(6)	7779(5)	957(4)	10(1)	1.659
O(7)	5893(6)	579(6)	1236(4)	11(1)	2.060

Table 3a. Selected interatomic distances (up to 3.01 Å) , bond angles and distortion parameters (QE: quadratic elongation, AV: angle variance) for $Sr_2Ga_2O_5$.

Sr(1)-O(1)	2.473(3)	Sr(1)-O(3)	2.529(3)
Sr(1)-O(3)	2.535(3)	Sr(1)-O(2)	2.543(3)
Sr(1)-O(4)	2.634(3)	Sr(1)-O(1)	2.677(3)
Sr(1)-O(5)	3.047(4)		

Sr(2)-O(1)	2.484(4)	Sr(2)-O(5)	2.570(4)
Sr(2)-O(4)	2.599(3)	Sr(2)-O(1)	2.622(4)
Sr(2)-O(2)	2.631(3)	Sr(2)-O(3)	2.633(3)
Sr(2)-O(3)	2.644(3)		

Ga(1)-O(3)	1.829(3)	Ga(1)-O(5)	1.830(3)
Ga(1)-O(4)	1.873(3)	Ga(1)-O(2)	1.881(3)
QE 1.012		AV 45.51	

Ga(2)-O(1)	1.823(4)	Ga(2)-O(4)	1.846(3)
Ga(2)-O(2)	1.870(3)	Ga(2)-O(5)	1.879(4)

QE	1.016	AV	58.09

O(3)-Ga(1)-O(5)	108.26(16)	O(3)-Ga(1)-O(4)	118.95(15)
O(5)-Ga(1)-O(4)	102.29(16)	O(3)-Ga(1)-O(2)	111.28(15)
O(5)-Ga(1)-O(2)	114.16(15)	O(4)-Ga(1)-O(2)	101.78(15)
O(1)-Ga(2)-O(4)	115.13(15)	O(1)-Ga(2)-O(2)	116.63(14)
O(4)-Ga(2)-O(2)	111.92(15)	O(1)-Ga(2)-O(5)	96.62(16)
O(4)-Ga(2)-O(5)	111.02(15)	O(2)-Ga(2)-O(5)	103.65(15)
Ga(2)-O(1)-Ga(1)	117.70(18)	Ga(2)-O(4)-Ga(1)	125.03(18)
Ga(1)-O(5)-Ga(2)	124.2(2)		

Table 3b. Selected interatomic distances (up to 3.01 Å) , bond angles and distortion parameters (QE: quadratic elongation, AV: angle variance) for $Sr_5Ga_6O_{14}$.

Sr(1)-O(5)	2.475(4)	Sr(1)-O(5)	2.475(4)
Sr(1)-O(3)	2.523(5)	Sr(1)-O(3)	2.523(5)
Sr(1)-O(6)	2.652(4)	Sr(1)-O(6)	2.652(4)
Sr(2)-O(7)	2.484(5)	Sr(2)-O(1)	2.626(5)
Sr(2)-O(3)	2.636(5)	Sr(2)-O(4)	2.639(4)
Sr(2)-O(6)	2.656(5)	Sr(2)-O(4)	2.802(5)
Sr(2)-O(7)	2.830(5)	Sr(2)-O(2)	3.009(5)
Sr(3)-O(7)	2.345(5)	Sr(3)-O(5)	2.368(5)

Sr(3)-O(2)	2.506(5)	Sr(3)-O(1)	2.597(5)
Sr(3)-O(6)	2.709(5)	Sr(3)-O(6)	2.782(5)
Sr(3)-O(2)	2.962(5)		

Ga(1)-O(4)	1.828(4)	Ga(1)-O(5)	1.843(4)
Ga(1)-O(1)	1.851(4)	Ga(1)-O(2)	1.858(5)
QE	1.006	AV	23.65

Ga(2)-O(7)	1.798(5)	Ga(2)-O(3)	1.833(4)
Ga(2)-O(4)	1.870(5)	Ga(2)-O(1)	1.874(4)
QE	1.006	AV	28.03

Ga(3)-O(6)	1.803(5)	Ga(3)-O(3)	1.855(4)
Ga(3)-O(2)	1.861(4)	Ga(3)-O(5)	1.884(4)
QE	1.023	AV	102.97

O(4)-Ga(1)-O(5)	108.6(2)	O(4)-Ga(1)-O(1)	116.8(2)
O(5)-Ga(1)-O(1)	107.3(2)	O(4)-Ga(1)-O(2)	113.5(2)
O(5)-Ga(1)-O(2)	104.1(2)	O(1)-Ga(1)-O(2)	105.7(2)

O(7)-Ga(2)-O(3)	114.1(2)	O(7)-Ga(2)-O(4)	112.1(2)
O(3)-Ga(2)-O(4)	103.6(2)	O(7)-Ga(2)-O(1)	115.6(2)
O(3)-Ga(2)-O(1)	105.9(2)	O(4)-Ga(2)-O(1)	104.3(2)

O(6)-Ga(3)-O(3)	120.5(2)	O(6)-Ga(3)-O(2)	118.7(2)
O(3)-Ga(3)-O(2)	99.6(2)	O(6)-Ga(3)-O(5)	114.1(2)
O(3)-Ga(3)-O(5)	97.6(2)	O(2)-Ga(3)-O(5)	102.8(2)
Ga(1)-O(1)-Ga(2)	112.3(2)	Ga(1)-O(2)-Ga(3)	120.1(2)
Ga(2)-O(3)-Ga(3)	127.8(3)	Ga(1)-O(4)-Ga(2)	111.9(2)
Ga(1)-O(5)-Ga(3)	121.6(2)		

Table 4a. Anisotropic displacement parameters ($Å^2$ x 10^3) for $Sr_2Ga_2O_5$. The anisotropic displacement factor exponent takes the form: $-2\pi^2$ [$h^2 a^{*2} U_{11}$ + ... + 2 h k a* b* U_{12}].

	U_{11}	U_{22}	U_{33}	U_{23}	U_{13}	U_{12}
Sr(1)	6(1)	7(1)	12(1)	2(1)	1(1)	1(1)
Sr(2)	6(1)	6(1)	9(1)	0(1)	1(1)	0(1)
Ga(1)	6(1)	6(1)	5(1)	0(1)	0(1)	-1(1)
Ga(2)	5(1)	6(1)	5(1)	0(1)	0(1)	-1(1)
O(1)	10(2)	10(2)	5(2)	-1(1)	-3(1)	1(2)
O(2)	6(2)	10(2)	8(2)	-1(2)	1(1)	-4(2)
O(3)	12(2)	5(2)	7(2)	0(1)	-2(2)	0(2)
O(4)	11(2)	7(2)	9(2)	-2(2)	0(1)	4(2)
O(5)	9(2)	13(2)	19(2)	-7(2)	6(2)	-5(2)

Table 4b. Anisotropic displacement parameters ($Å^2$ x 10^3) for $Sr_5Ga_6O_{14}$. The anisotropic displacement factor exponent takes the form: $-2\pi^2$ [$h^2a^{*2}U_{11}$ + ... + 2 h k a* b* U_{12}].

	U_{11}	U_{22}	U_{33}	U_{23}	U_{13}	U_{12}
Sr(1)	20(1)	15(1)	9(1)	7(1)	5(1)	8(1)
Sr(2)	8(1)	9(1)	8(1)	1(1)	0(1)	1(1)
Sr(3)	15(1)	15(1)	13(1)	-4(1)	1(1)	-1(1)
Ga(1)	7(1)	5(1)	5(1)	0(1)	1(1)	-1(1)
Ga(2)	7(1)	5(1)	7(1)	1(1)	1(1)	0(1)
Ga(3)	6(1)	5(1)	4(1)	0(1)	0(1)	0(1)
O(1)	15(3)	8(2)	9(2)	2(2)	2(2)	-3(2)
O(2)	23(3)	7(2)	8(2)	2(2)	-1(2)	-6(2)
O(3)	10(2)	11(2)	9(2)	-1(2)	3(2)	5(2)
O(4)	10(2)	14(2)	6(2)	3(2)	0(2)	4(2)
O(5)	7(2)	15(2)	5(2)	1(2)	2(2)	4(2)
O(6)	14(3)	11(2)	5(2)	-1(2)	1(2)	1(2)
O(7)	11(2)	14(2)	7(2)	1(2)	-1(2)	3(2)

A single tetrahedral layer and the location of the Sr-cations directly above the sheet in high-pressure $Sr_5Ga_6O_{14}$.

Highlights

- We report the crystal structures of two new strontium oxogallates with composition $Sr_2Ga_2O_5$ and $Sr_5Ga_6O_{14}$
- Both phases have been obtained in the course of high-pressure piston-cylinder experiments performed at 1.5 and 3.0 GPa
- The crystallochemical characteristics and similarities with known structure types are discussed in detail

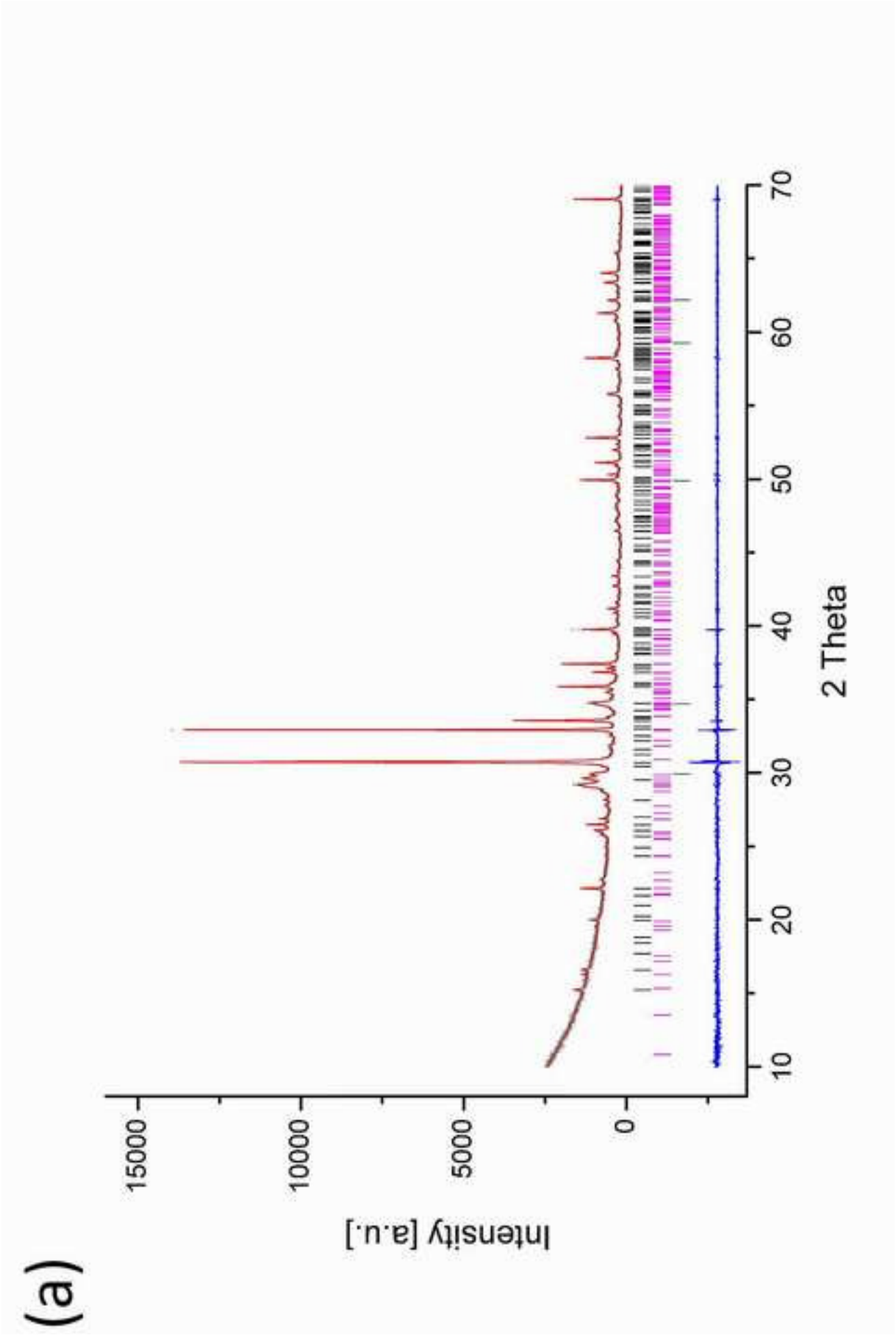

Figure(s)

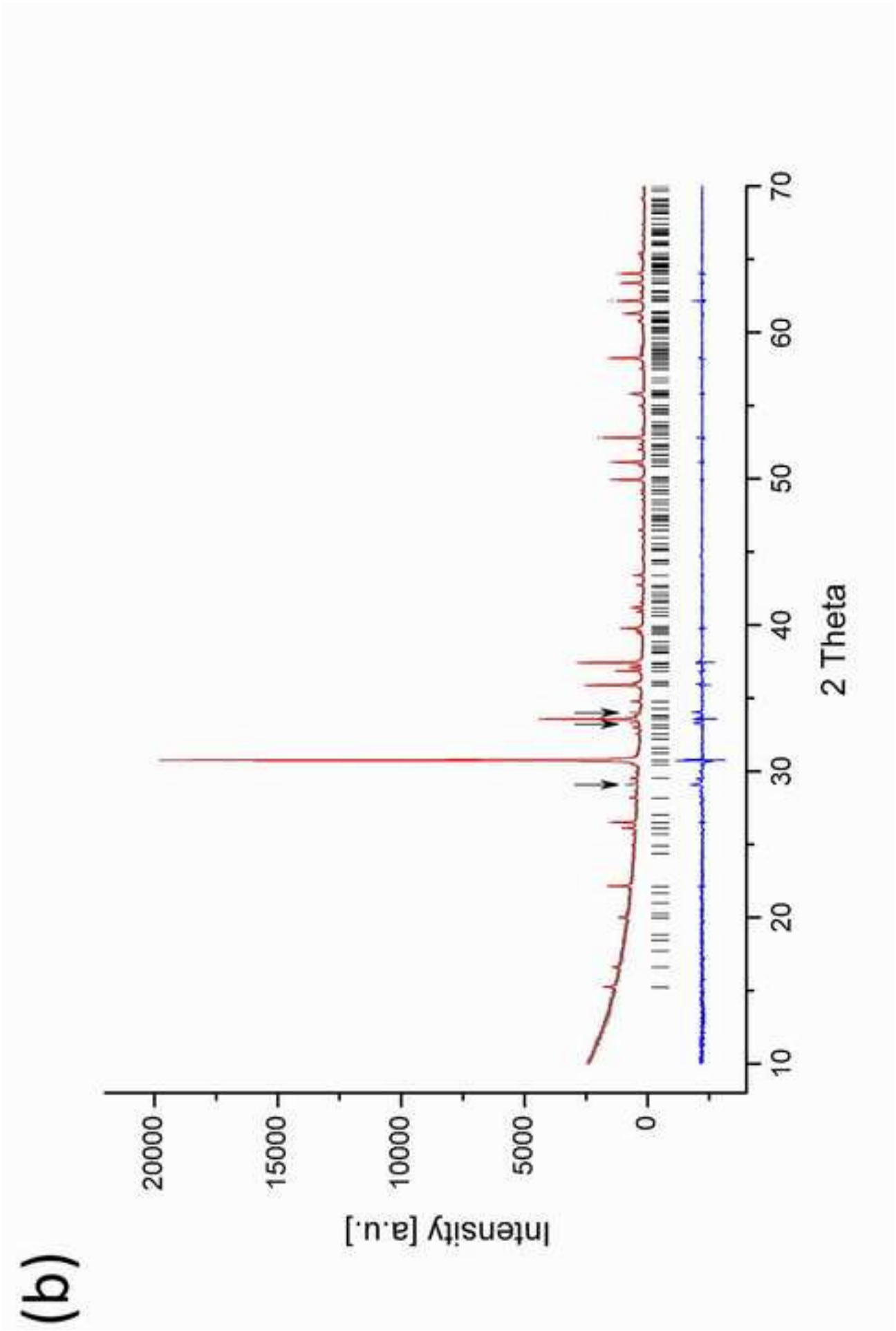

Figure_1b_revised

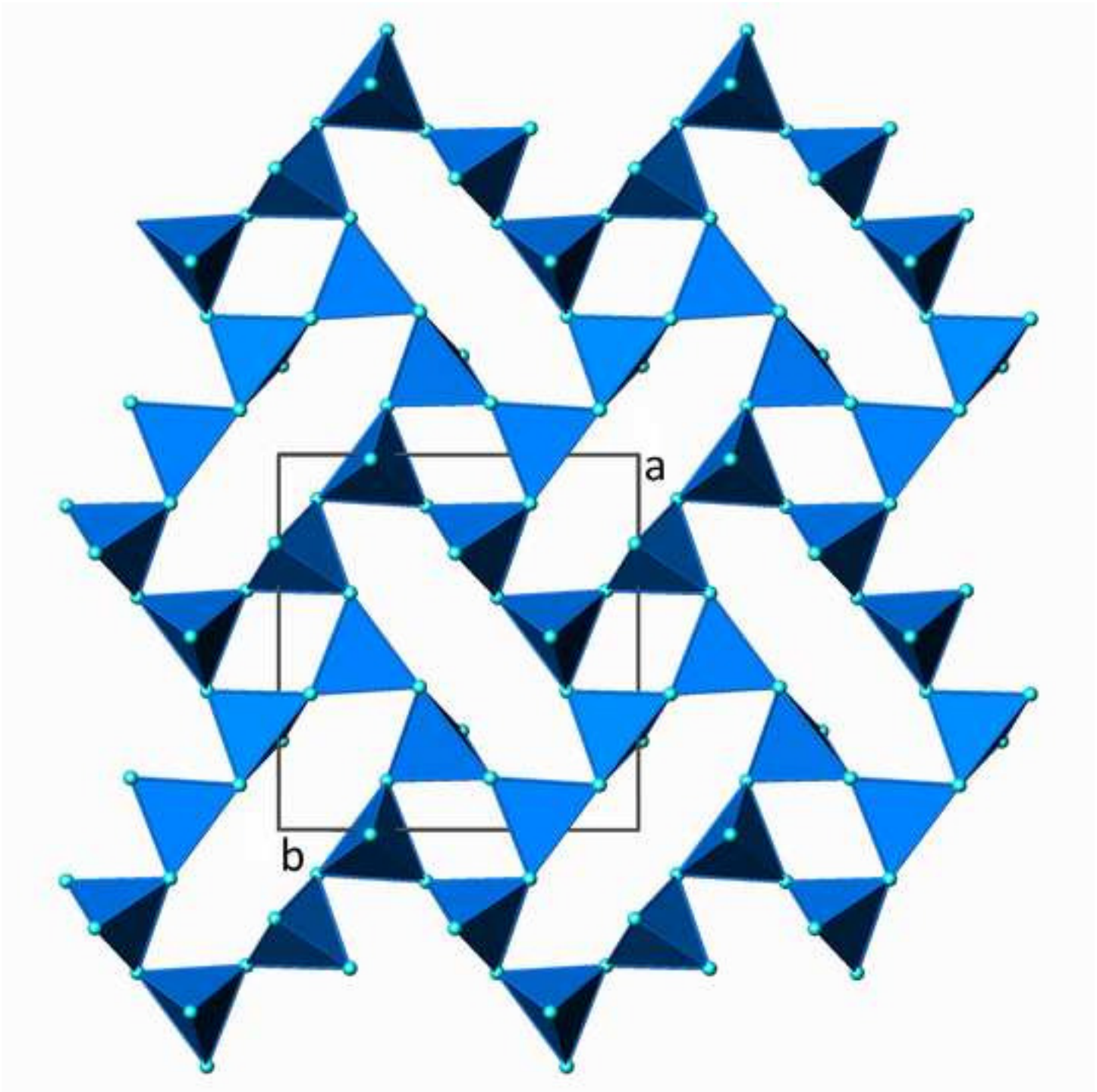

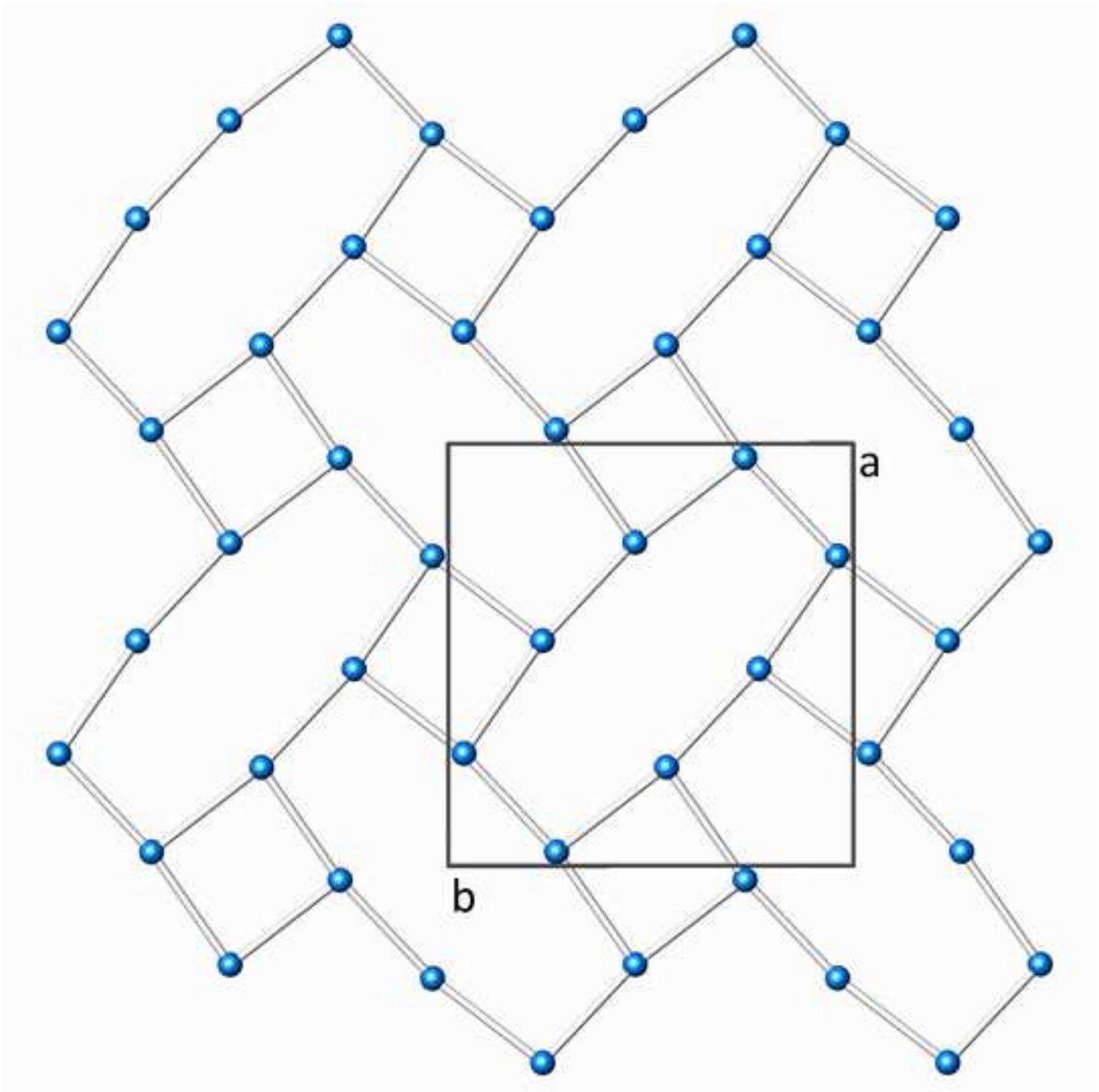

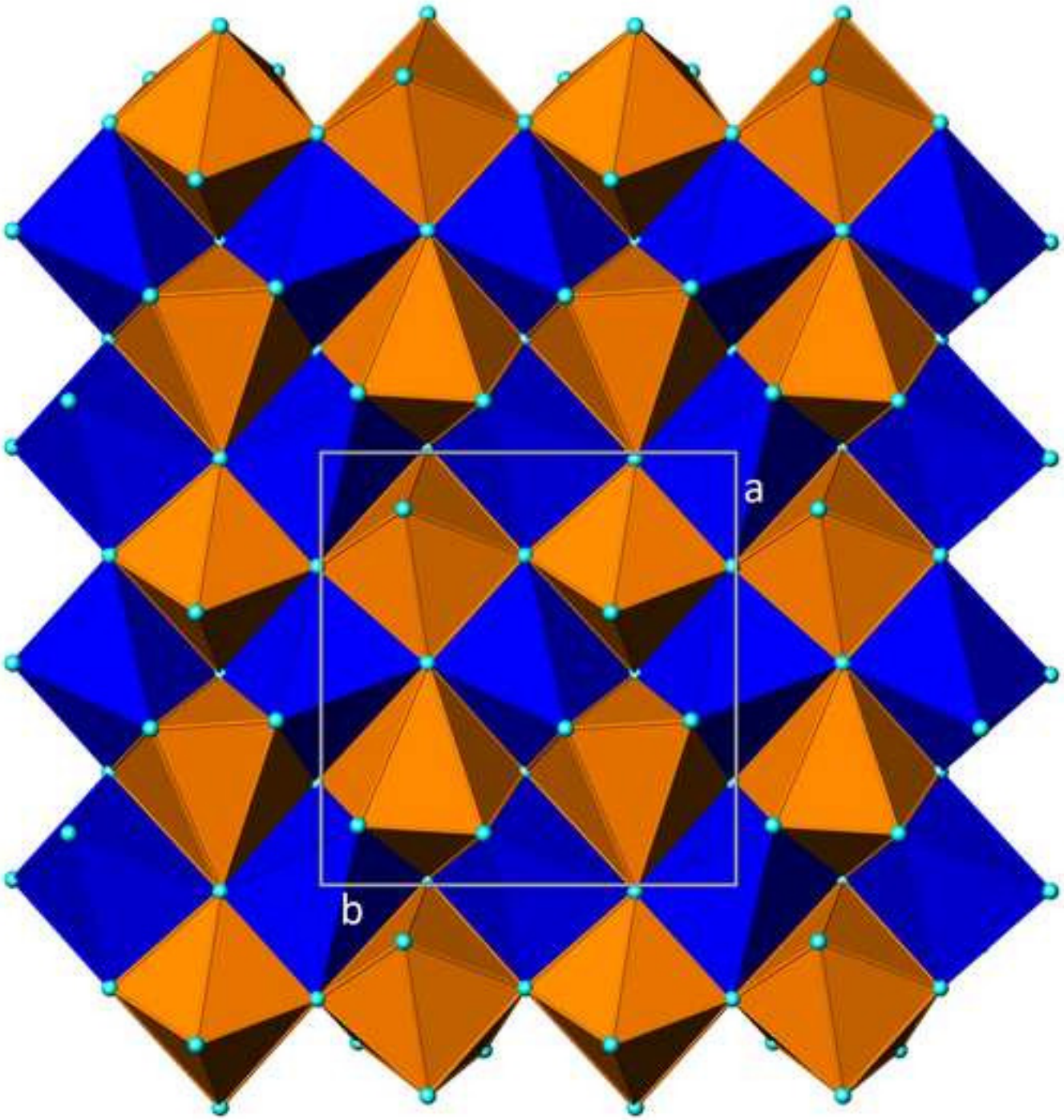

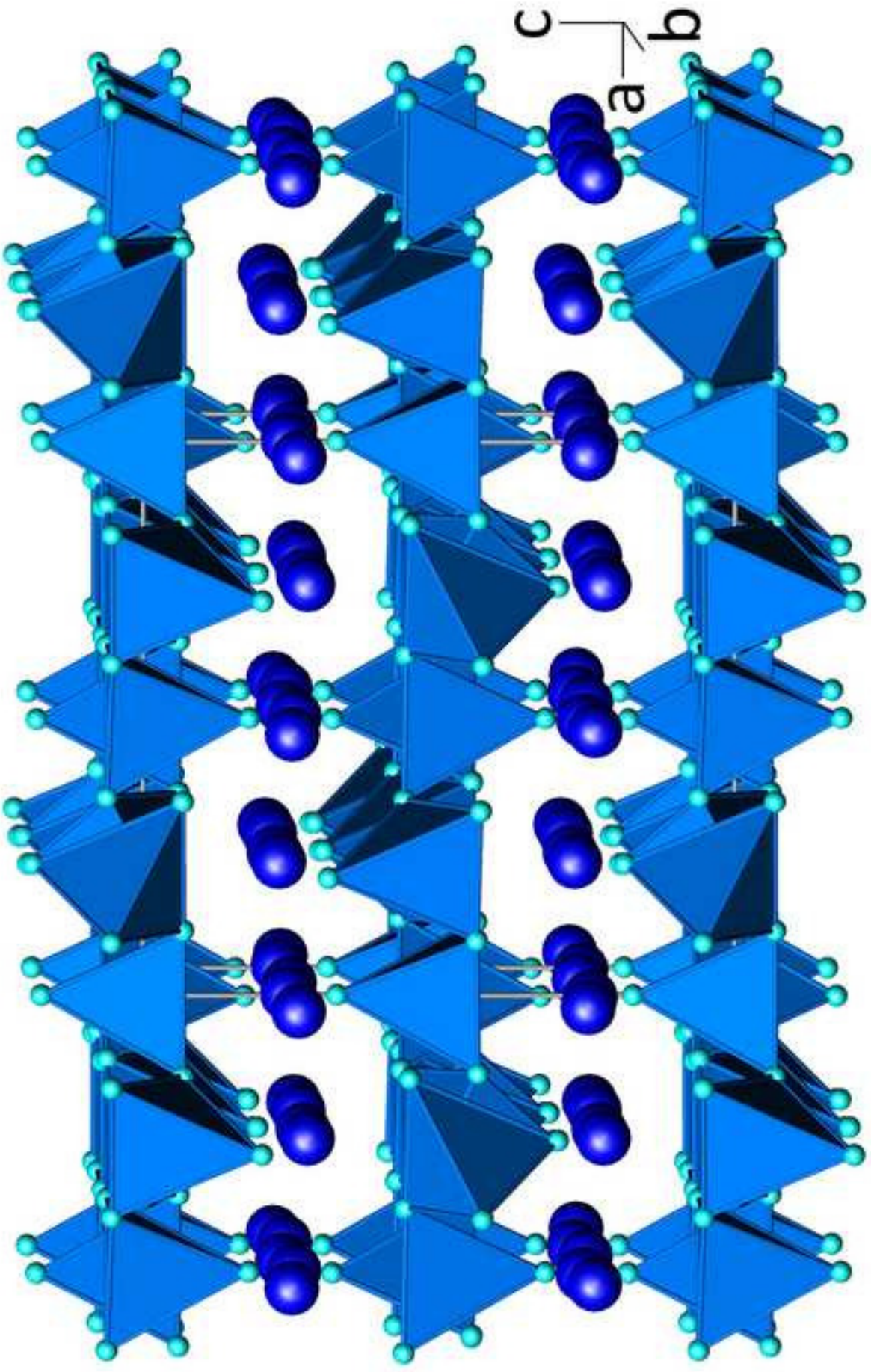

Figure_5

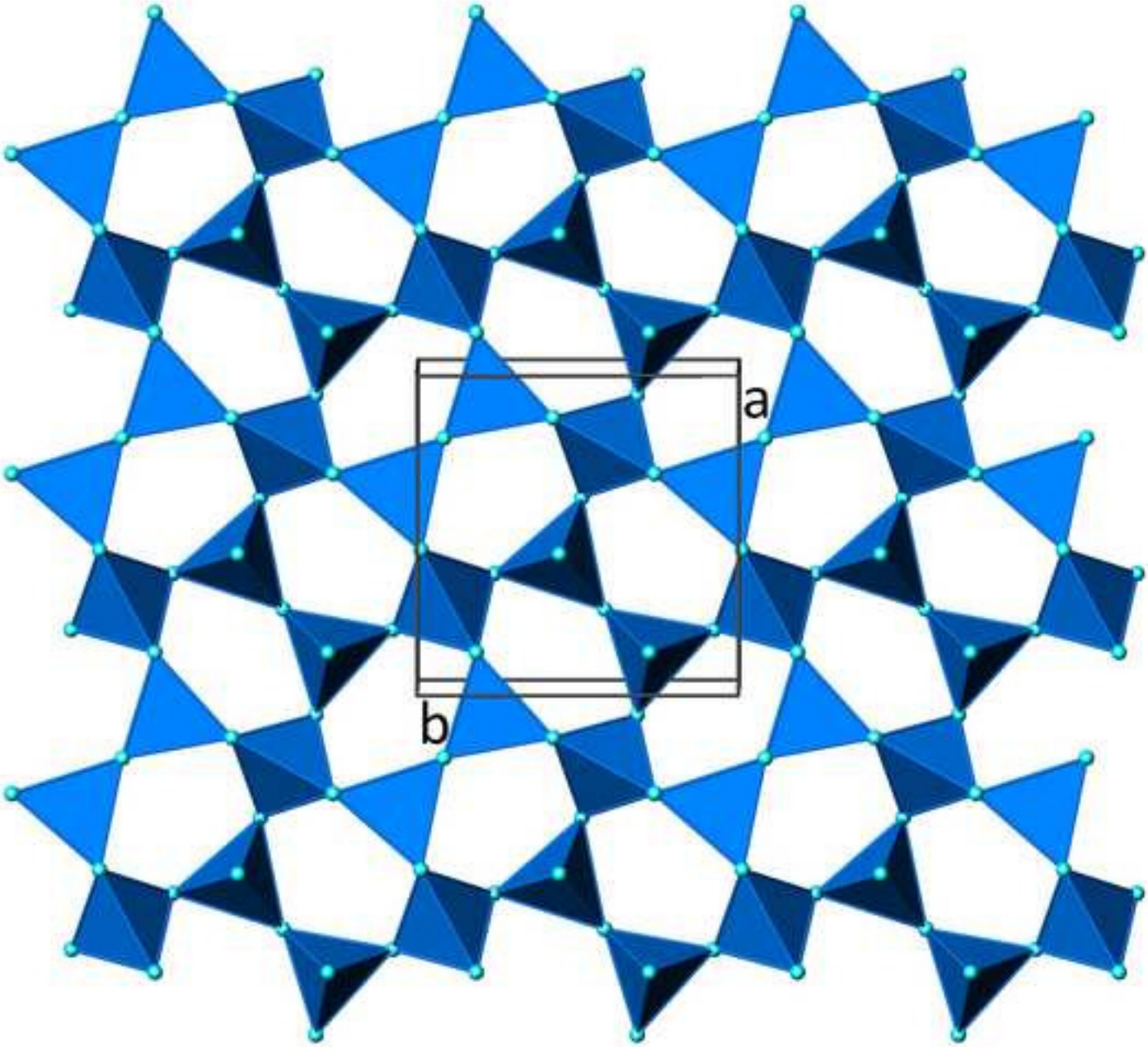

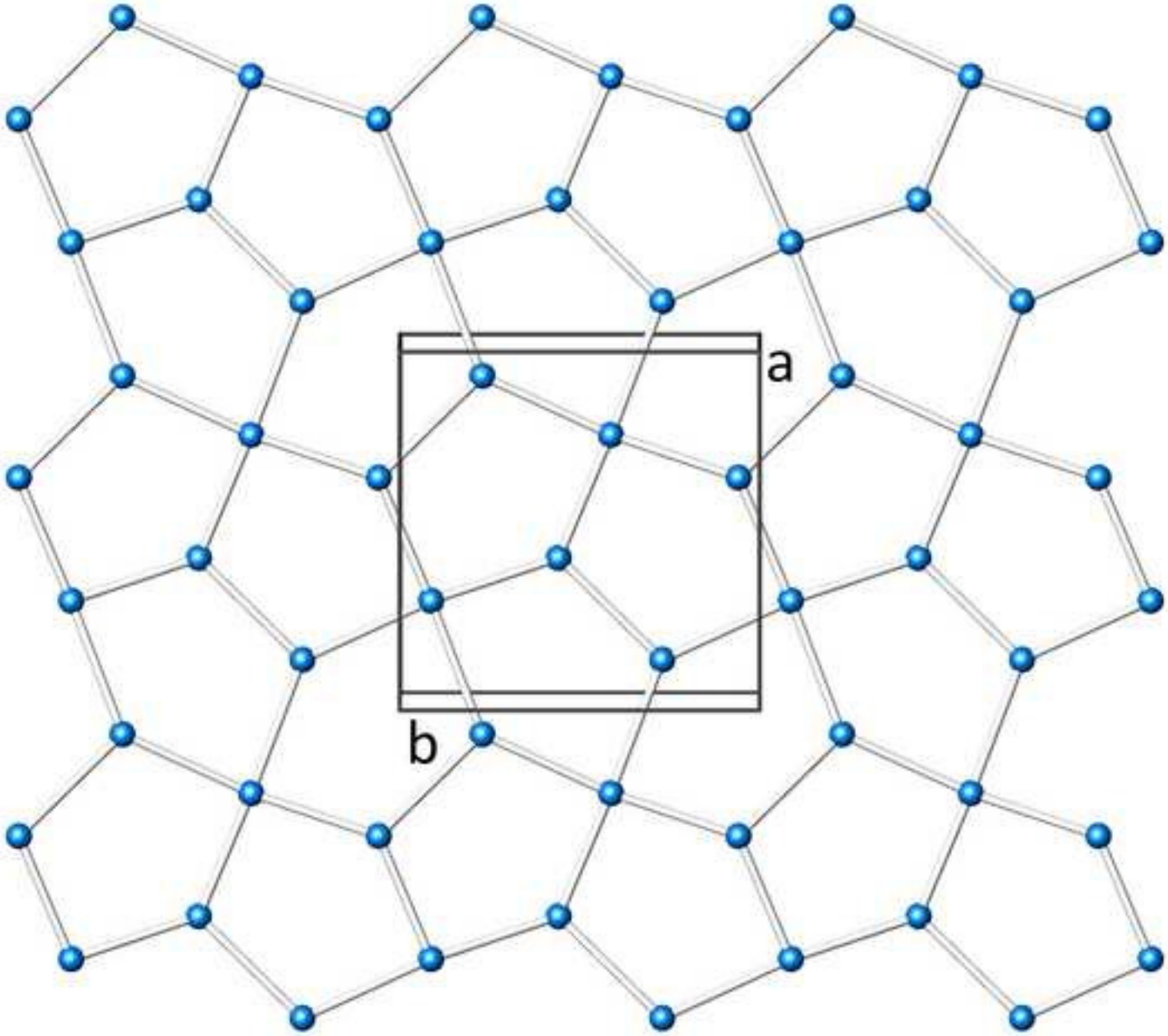

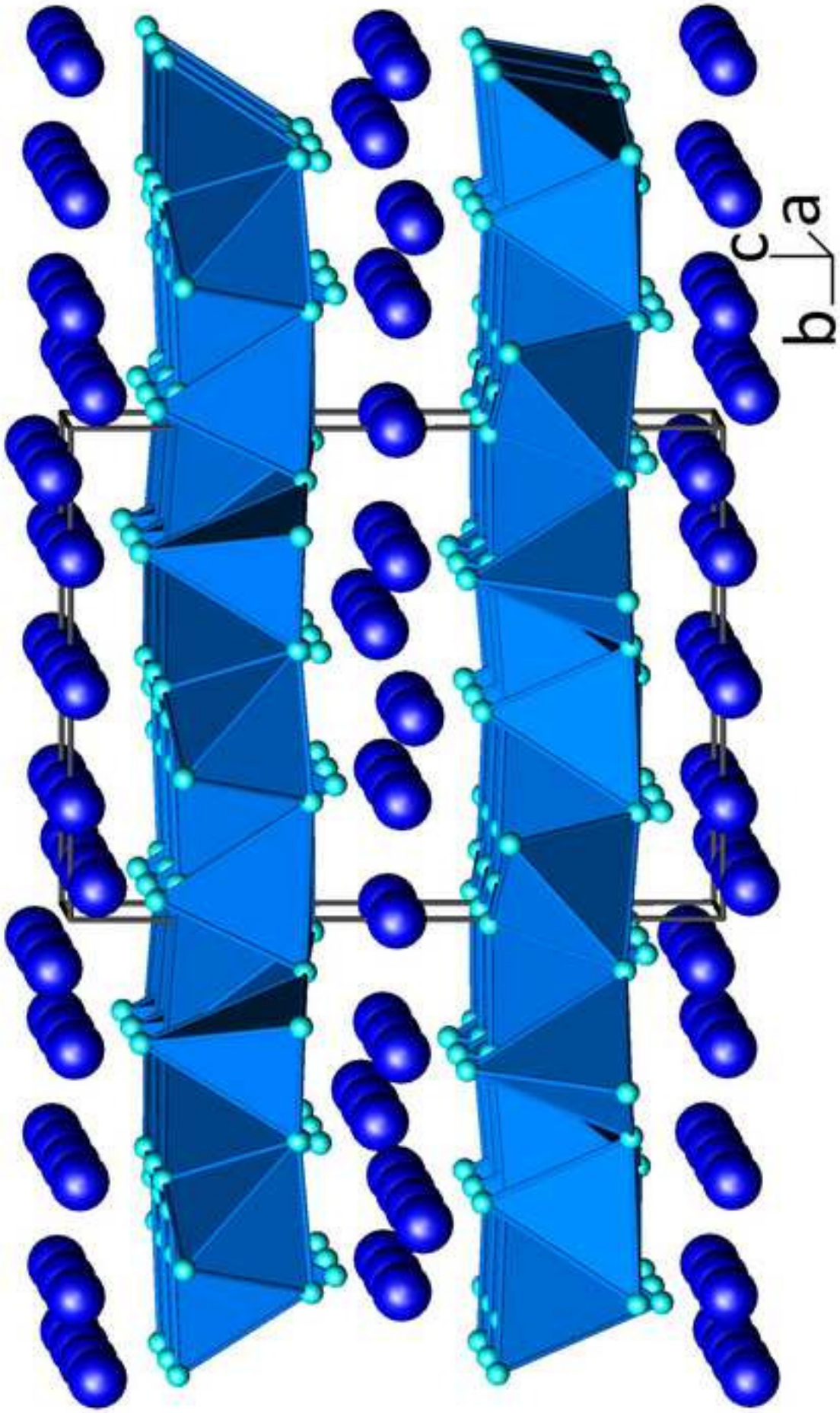

Figure_8

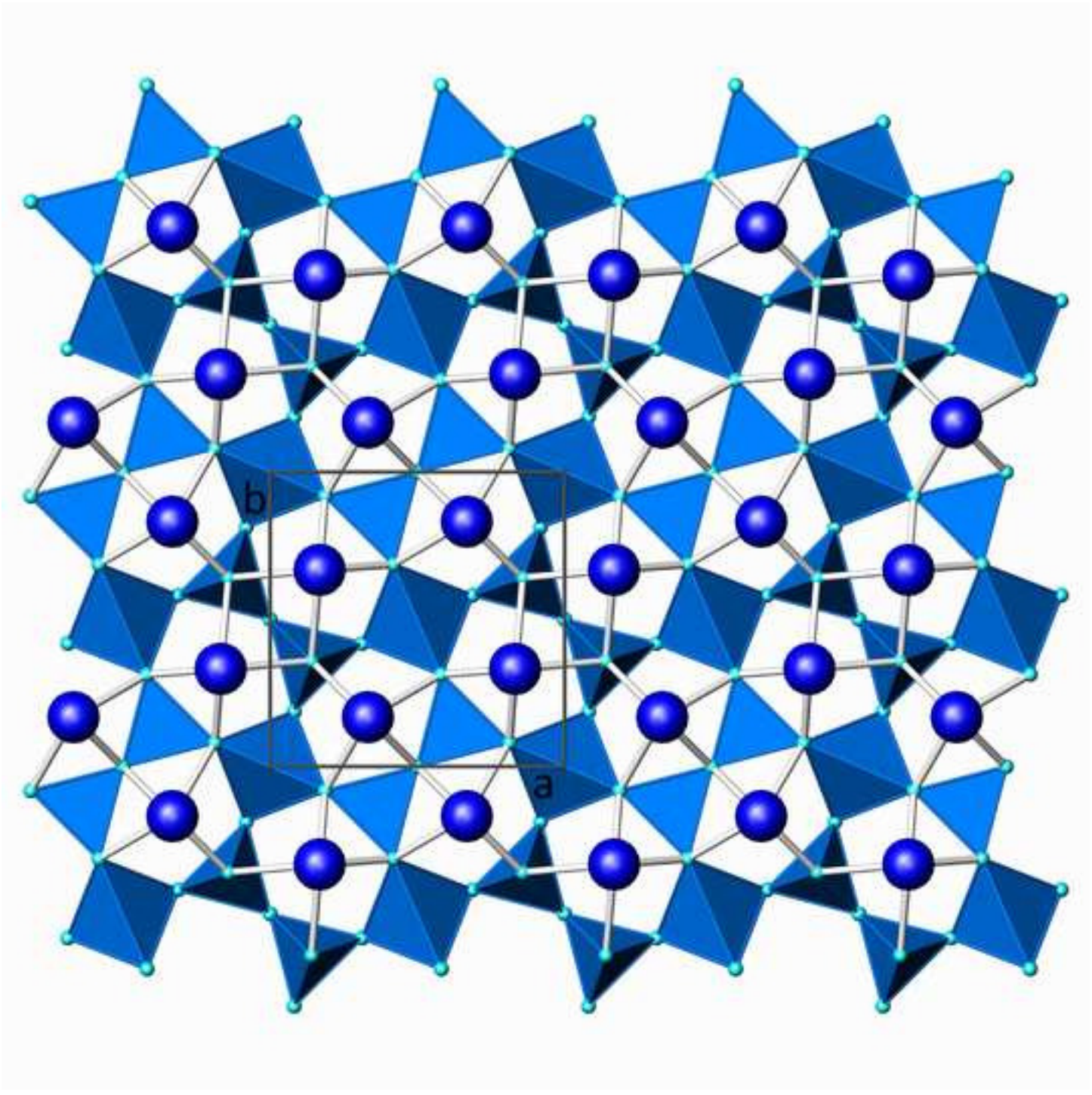

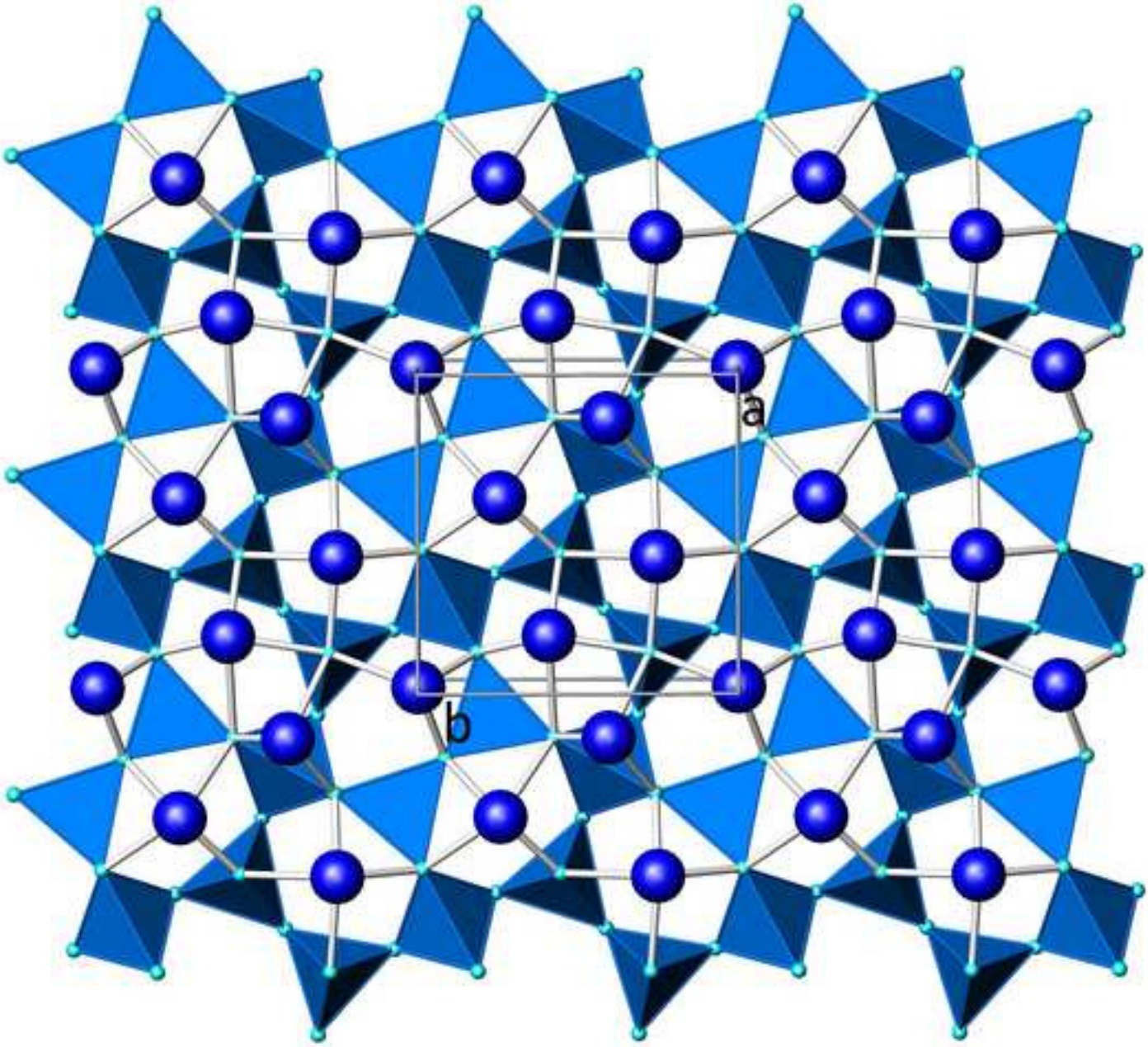

Figure_9c

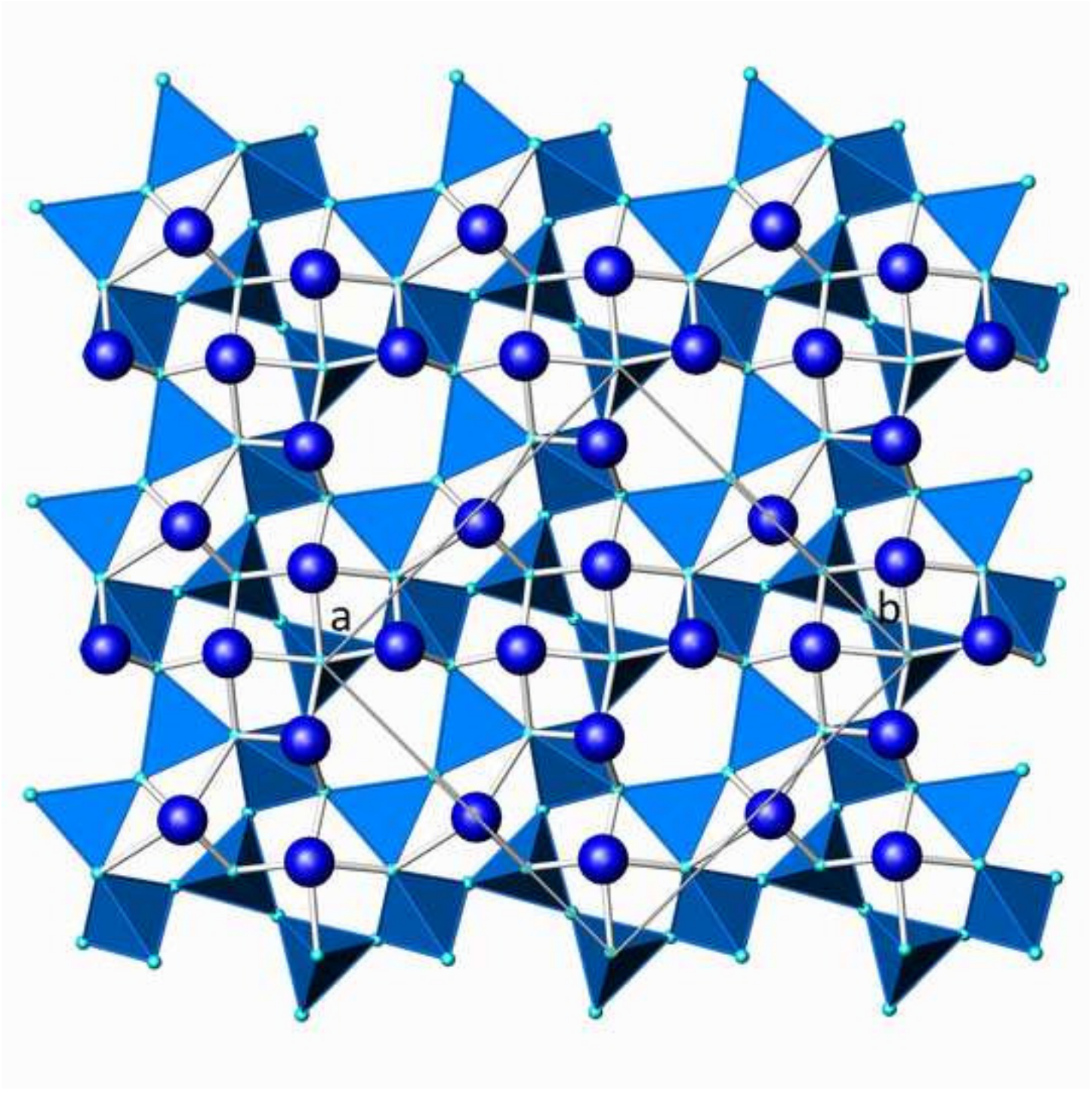

*Graphical Abstract (TOC Figure)

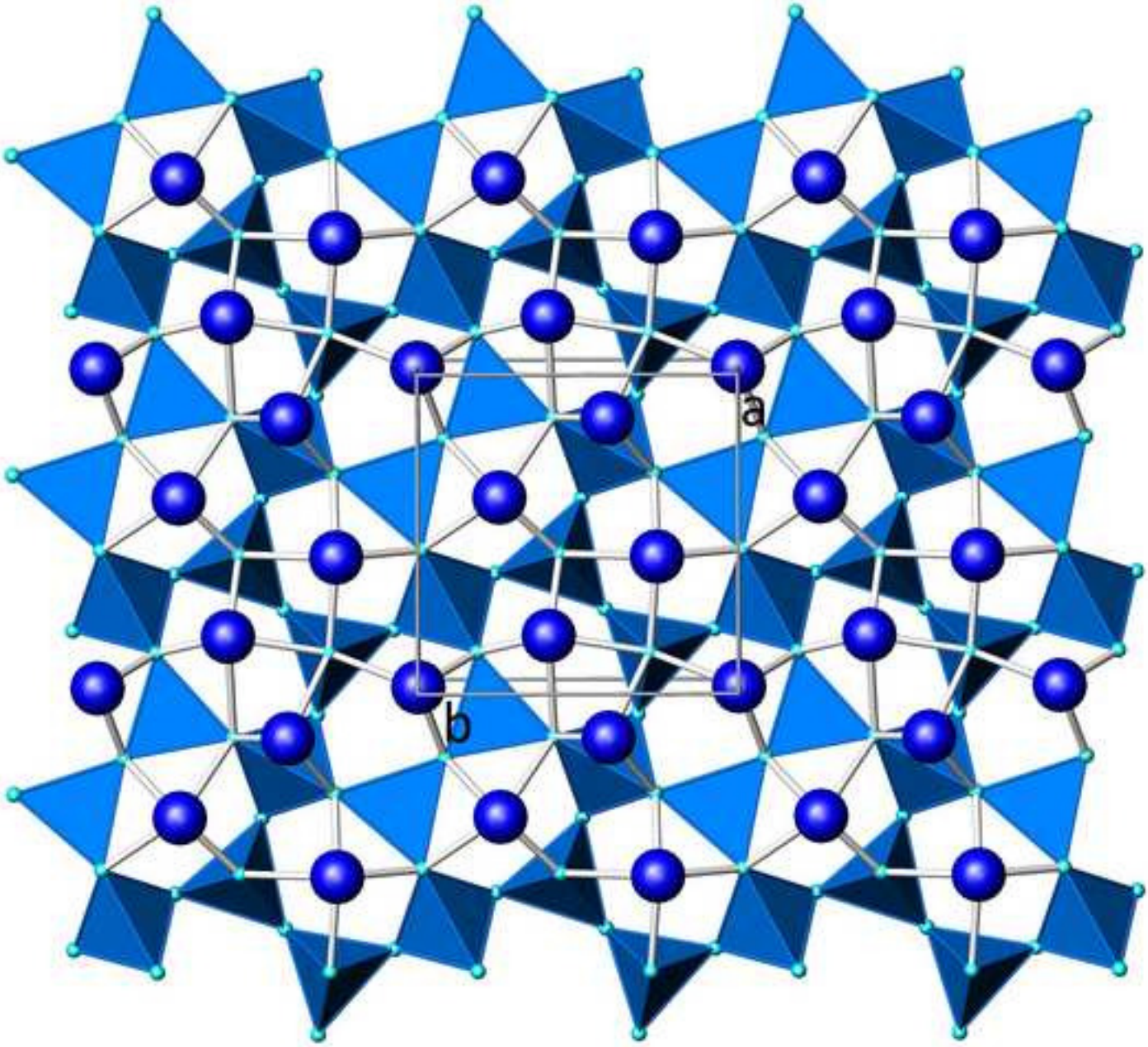

A single tetrahedral layer and the location of the Sr-cations directly above the sheet in high-pressure $Sr_5Ga_6O_{14}$.